

Fingerprints of climatic changes through the late Cenozoic in southern Asian flora: *Magnolia* section *Michelia* (Magnoliaceae)

Nan Zhao^{1,2,†}, Suhyeon Park^{3,†}, Yu-Qu Zhang⁴, Ze-Long Nie⁵, Xue-Jun Ge¹, Sangtae Kim^{3,*} and Hai-Fei Yan^{1,*}

¹Key Laboratory of Plant Resources Conservation and Sustainable Utilization, South China Botanical Garden, Chinese Academy of Sciences, Guangzhou 510650, China, ²University of Chinese Academy of Sciences, Beijing 100049, China, ³Department of Biotechnology, Sungshin Women's University, Seoul 01133, Republic of Korea, ⁴College of Pharmacy, Shaanxi University of Chinese Medicine, Xi'an 712046, China and ⁵Key Laboratory of Plant Resources Conservation and Utilization, College of Biology and Environmental Sciences, Jishou University, Jishou 416000, China

*For correspondence. E-mail: yanhaifei@scbg.ac.cn or amborella@sungshin.ac.kr

†These authors contributed equally to this work.

Received: 22 January 2022 Returned for revision: 2 April 22 Editorial decision: 19 April 2022 Accepted: 21 April 2022

• **Background and Aims** Ongoing global warming is a challenge for humankind. A series of drastic climatic changes have been proven to have occurred throughout the Cenozoic based on a variety of geological evidence, which helps to better understand our planet's future climate. Notably, extant biomes have recorded drastic environmental shifts. The climate in southern Asia, which hosts high biodiversity, is deeply impacted by the Asian monsoon. The origins and evolutionary dynamics of biomes occurring between the tropics and sub-tropics in southern Asia have probably been deeply impacted by climatic changes; however, these aspects remain poorly studied. We tested whether the evolutionary dynamics of the above biomes have recorded the drastic, late Cenozoic environmental shifts, by focusing on *Magnolia* section *Michelia* of the family Magnoliaceae.

• **Methods** We established a fine time-calibrated phylogeny of *M.* section *Michelia* based on complete plastid genomes and inferred its ancestral ranges. Finally, we estimated the evolutionary dynamics of this section through time, determining its diversification rate and the dispersal events that occurred between tropical and sub-tropical areas.

• **Key Results** The tropical origin of *M.* section *Michelia* was dated to the late Oligocene; however, the diversification of its core group (i.e. *M.* section *Michelia* subsection *Michelia*) has occurred mainly from the late Miocene onward. Two key evolutionary shifts (dated approx. 8 and approx. 3 million years ago, respectively) were identified, each of them probably in response to drastic climatic changes.

• **Conclusion** Here, we inferred the underlying evolutionary dynamics of biomes in southern Asia, which probably reflect late Cenozoic climatic changes. The occurrence of modern Asian monsoons was probably fundamental for the origin of *M.* section *Michelia*; moreover, the occurrence of asymmetric dispersal events between the tropics and sub-tropics hint at an adaptation strategy of *M.* section *Michelia* to global cooling, in agreement with the tropical conservatism hypothesis.

Key words: Biological interchanges, global warming, Magnoliaceae, section *Michelia*, sub-tropics, tropics.

INTRODUCTION

Humans are facing global warming, which has been caused by an increase of human-made greenhouse gas emissions since the start of the industrial era (Hansen *et al.*, 1998) and is posing a major threat to biodiversity (Dawson *et al.*, 2011). Understanding the effects of past climatic changes could help us to learn about future biodiversity. During the Cenozoic era, corresponding to the past 65 million years, a series of drastic climatic changes (Guo *et al.*, 2008; Beerling and Royer, 2011) have occurred. These trends have been reconstructed based on both geological (An *et al.*, 2001; Zachos *et al.*, 2001; Guo *et al.*, 2002; Westerhold *et al.*, 2020) and paleontological evidence (Cerling *et al.*, 1997; Sun and Wang, 2005).

The Asian continent has experienced complex and continuous environmental changes (e.g. the occurrence of monsoon climate and inland aridity) during the Cenozoic era (Guo

et al. 2008), which have been exacerbated by the uplift of the Himalaya and Tibetan plateau since the Eocene (Liu *et al.*, 2015; Li *et al.*, 2021). Other factors (e.g. the retreat of the Paratethys Sea, the opening of the South China Sea and the decrease of atmospheric CO₂ concentration) have also progressively affected this climatic evolution (Ramstein *et al.*, 1997; Licht *et al.*, 2014). Monsoon systems are among the most specific Asian climatic systems. Modern Asian monsoon systems have probably originated in the late Oligocene–Early Miocene [25–22 million years ago (Ma)], although monsoon-like climates in Asia have occurred since the Eocene (but were mainly restricted to southern Asia) (Guo *et al.*, 2008; Licht *et al.*, 2014; Spicer, 2017; Spicer *et al.*, 2017; Su *et al.*, 2020; Bhatia *et al.*, 2021; Wambulwa *et al.*, 2021).

Drastic paleoenvironmental changes have occurred in Asia especially in the late Cenozoic. For example, the modern East Asian monsoon system strengthened approx. 8 Ma after being

established: around the Oligocene–Miocene boundary (approx. 22 Ma) (Guo *et al.*, 2002; Sun and Wang, 2005). Afterwards, it weakened, and has intensified again since the Plio–Pleistocene transition (approx. 3 Ma) (Wang, 2004; Clift *et al.*, 2014). In the meanwhile, our planet has experienced global cooling, which has resulted in a late Miocene carbon isotope shift (7–8 Ma, related to major changes in the carbon cycle) and the Plio–Pleistocene transition (driven by the entire establishment of ice sheets in the Northern Hemisphere) (Westerhold *et al.*, 2020). Accordingly, there was a temporary coupling of the atmosphere–ice sheet–tectonic movements in Asia over the Cenozoic era (Liu *et al.*, 1998; Tada *et al.*, 2016).

The dynamics of the global and Asian monsoon climates (and/or mountain orogeny) have probably been the cause of high biodiversity, rapid diversification and biological interchanges in Asia (Spicer, 2017; Kong *et al.*, 2017, 2022; Spicer *et al.*, 2017; Xing and Ree, 2017; Yu *et al.*, 2017; Ding *et al.*, 2020). Meanwhile, the evolutionary history of extant biomes could reflect past climatic changes at different time scales (Arakaki *et al.*, 2011; Klaus *et al.*, 2016; Xing and Ree, 2017; Ding *et al.*, 2020; Kong *et al.*, 2022). For example, previous studies have found that the evolutionary history of biota (flora or fauna) in the Tibet–Himalaya–Hengduan region in Asia is genetically linked to the uplift of mountains in this same region and to the intensification of the Asian monsoon (Klaus *et al.*, 2016; Xing and Ree, 2017; Ding *et al.*, 2020; Xu *et al.*, 2020).

With the term ‘Southern Asia’ we refer to Asian tropical and sub-tropical regions at low latitudes (<32°N) that are deeply influenced by the Asian monsoon systems [i.e. the East Asian Monsoon (EAM), the South Asian Monsoon (SAM) and the Western North Pacific Monsoon (WNPM)] (Wang and Ho, 2002; Spicer *et al.*, 2017). These regions host incredible biodiversity, the largest evergreen broad-leaved forest (EBLF) in the world (Song and Da, 2016), several biodiversity hotspots (Myers *et al.*, 2000; Ying, 2001) (e.g. Indo-Burma, South-Central China, Nanling, Sundaland, and the Philippines) and the refugia of many relict plants (Qiu *et al.*, 2011; Tang *et al.*, 2018). Notably, southern Asia seems to be the main source of the total floristic diversity of East Asia (Axelrod *et al.*, 1996; Qian, 2002). A recent study found that 9 % of the East Asian flora (mainly in the sub-tropics of southern Asia) have a tropical Asian origin (Chen *et al.*, 2017), indicating the importance of biological interchanges between the tropics and sub-tropics in southern Asia. Despite the importance of biodiversity in southern Asia, the local flora’s origin and evolutionary dynamics have not yet been well studied.

Under the theory of niche conservatism (Wiens and Donoghue, 2004; Wiens and Graham, 2005), asymmetries in both the *in situ* diversification rate and the migration directions are expected between the source (i.e. mild environment) and sink (i.e. harsh environment) in the context of climatic changes (i.e. global cooling and Asian monsoon development through the Cenozoic). Southern Asia is a good model for examining the imprints of the evolutionary dynamics of biomes, especially since this region was impacted by the cooling of global climate, the intensification of Asian monsoons and the Pleistocene climate oscillations. For taxa that originated in tropical areas, we should expect a gradual decrease in the number of dispersal events from the tropics to the sub-tropics, but an increase in the opposite direction in response to the establishment of harsh

conditions (i.e. cool and/or arid climate). To our knowledge, there is still little information on the detailed evolutionary dynamics (e.g. biotic interchanges and *in situ* diversification rates) that have occurred between the tropics and the sub-tropics in southern Asia.

In this study, we investigated whether the evolutionary dynamics of *Magnolia* section *Michelia* (L.) Baill. of the family Magnoliaceae reflect the drastic environmental shifts that have occurred in the late Cenozoic. *Magnolia* section *Michelia* includes four subsections according to the classification system of Figlar and Nootboom (2004): subsection *Michelia* (L.) Figlar & Noot., subsection *Elmerrillia* (Dandy) Figlar & Noot., subsection *Maingola* Figlar & Noot. and subsection *Aromadendron* Figlar & Noot. The group contains a total of approx. 73 species, all distributed in southern Asia (i.e. tropical and sub-tropical forests in East Asia, Indochina, southern India, Sri Lanka and the Malay Archipelago, Xia *et al.*, 2008; www.magnoliasociety.org; Fig. 1). As the core group in *M.* section *Michelia*, subsection *Michelia* has the highest species richness (it includes 57 species) and is distributed in both tropical and (mainly) sub-tropical southern Asia. The other three subsections are instead mainly distributed in tropical areas of southern Asia. A robust backbone phylogeny of the Magnoliaceae has been recently reconstructed based on plastid genomes and nuclear single nucleotide polymorphisms (SNPs) (Y. Wang *et al.*, 2020; Dong *et al.*, 2022), demonstrating that *M.* section *Michelia* is closely related to *Magnolia* section *Yulania* (Spach) Dandy, and that both belong to *Magnolia* subgenus *Yulania* (Y. Wang *et al.*, 2020). Additionally, based on previous dating results, *M.* section *Michelia* should have been strongly impacted by late Cenozoic environmental changes (Nie *et al.*, 2008; Dong *et al.*, 2022).

With the rapid growth of genomic data, the incongruence between nuclear and plastid trees has increasingly become clearer through plastid capture via (ancient or recent) hybridization or introgression (Wang *et al.*, 2021; Dong *et al.*, 2022): the analysis of plastid DNA can provide a more detailed evolutionary history than that of nuclear data alone (e.g. Baldwin *et al.* 2021). Here, we established a fully resolved phylogeny for *M.* section *Michelia* based on whole plastid genomes and a dense taxon sampling (i.e. considering 37 species belonging to the section). Then, the evolutionary dynamics were analysed by multiple phylogenetic approaches: we tested whether the evolutionary history of this section reflects past climatic changes. Specifically, we (1) reconstructed the phylogeny, ages and ancestral ranges of *M.* section *Michelia*, (2) investigated the diversification rate and dispersal event patterns of the section throughout its evolutionary history and (3) inferred the potential causes for its dynamic patterns. The results of this case study were expected to shed light on the underlying evolutionary patterns of biodiversity in southern Asia and their past environmental driving forces.

MATERIALS AND METHODS

Taxon sampling

We sampled 96 accessions assigned to the genera *Magnolia* and *Liriodendron*, of which 41 were newly collected in this study (Supplementary data Table S1). Among the sampled accessions, we identified 37 species belonging to *M.* section

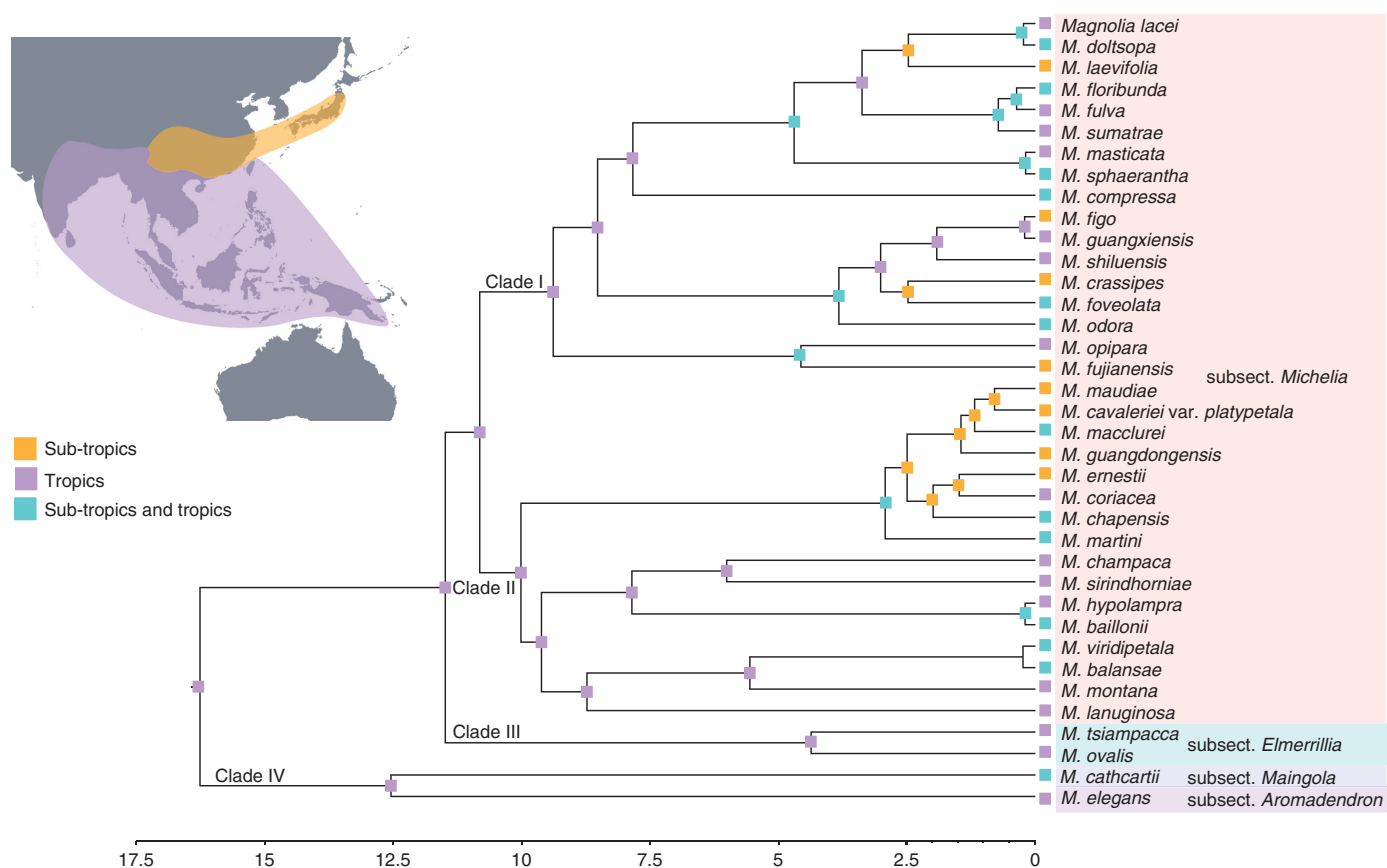


FIG. 1. Divergence time estimation for *Magnolia* section *Michelia* and reconstruction of the ancestral distribution area through the BioGeoBEARS package in RASP (Yu *et al.*, 2015). The inset map shows the biogeographical areas of *Magnolia* section *Michelia*.

Michelia. A limited number of taxa belonging to three small groups (i.e. *M.* section *Michelia* subsections *Elmerrillia*, *Maingola* and *Aromadendron*) were sampled; nevertheless, 42 accessions represented 33 taxa of *M.* section *Michelia* subsection *Michelia*. Notably, we only considered validly published species belonging to *M.* section *Michelia*. The richness of species belonging to this section in each area and their sampling fractions are summarized in Table 1.

Genome sequencing, plastid genome assembly and annotation

Total genomic DNA was extracted from the silica-dried leaf material of each sampling through the modified cetyltrimethylammonium bromide (CTAB) method (Porebski *et al.*, 1997). Paired-end (PE) Illumina sequencing libraries were constructed and sequenced on an Illumina HiSeq 2500 platform (Illumina, San Diego, CA, USA) and MGISEQ-2000 (MGI, Shenzhen, China) at the Beijing Genomics Institution (BGI, Wuhan, China). Two methods were used for the plastid genome assembly. In one case, the clean PE reads were mapped against the publicly available plastid genome of *Magnolia odora* (Chun) Figlar & Noot. (GenBank accession no. JX280398) using BWA v0.7.15 (Li and Durbin, 2009) and SAMtools v1.5 (Li *et al.*, 2009) to generate consensus sequences. In the other case, the clean PE reads were used to assemble the plastid genome in NOVOPlasty v2.5.9 (Dierckx *et al.*, 2017)

using a seed-and-extend algorithm. The consensus sequences obtained by the above two methods were checked by carrying out a new mapping with clean PE reads using Geneious v11.0.4 (Kearse *et al.*, 2012). Unexpected degenerate bases in the sequence were manually adjusted to generate the complete plastomes.

The assembled plastome sequences were annotated using the online program GeSeq (<https://chlorobox.mpimp-golm.mpg.de/geseq.html>; Tillich *et al.*, 2017). The positions of the start and stop codons and of the exon–intron boundaries were determined manually based on their alignments against the plastome of *M. odora* in MAFFT v7.407 (Katoh and Standley, 2013). Furthermore, the tRNA genes were annotated using ARAGORN (Laslett and Canback, 2004).

Phylogenetic reconstruction

Seventy-nine protein-coding genes and 89 non-coding regions (corresponding to 12 introns and 77 intergenic regions) of protein-coding genes were extracted from the assembled plastomes and aligned separately using MAFFT v7.407 (Katoh and Standley, 2013) under default settings. The aligned sequences and non-coding regions were hence concatenated. The best-fitting substitution models for each dataset were evaluated with PartitionFinder v2.1.1 (Lanfear *et al.*, 2017) under the corrected Akaike information criterion (AICc). Maximum

TABLE 1. Species richness within *Magnolia* section *Michelia* in the tropics and sub-tropics

Groups	Species richness (sampled species)	Distribution		Stem age	Crown age
		Tropics (sampled species)	Sub-tropics (sampled species)		
Section <i>Michelia</i>	73 (37)	61 (28)	24 (21)	25.52	16.26
Subsection <i>Michelia</i>	57 (33)	45 (24)	24 (20)	11.49	10.82
Subsection <i>Elmerrillia</i>	4 (2)	4 (2)	0 (0)	11.49	4.37
Subsection <i>Maingola</i>	7 (1)	7 (1)	1 (1)	12.54	No data
Subsection <i>Aromadendron</i>	5 (1)	5 (1)	0 (0)	12.54	No data

likelihood (ML) analyses were conducted in RAxML v8.2.1 (Stamatakis, 2014) with a rapid bootstrap (BS) of 1000 replicates. Additionally, Bayesian inference (BI) analyses were performed with MrBayes v3.2.6 according to the best PartitionFinder scheme (Ronquist et al., 2012). In these analyses, two Markov chain Monte Carlo (MCMC) runs, each with four chains (i.e. three heated and one cold), were conducted for 10 million generations. Each run began with one random tree, and the trees were sampled every 1000 generations. The convergence was assessed using TRACER v1.7.1 (Rambaut et al., 2018), considering effective sample size (ESS) values >200. The first 25 % of trees of each run were discarded as burn-in, while the remainder were used to calculate the consensus topology and the posterior probability (PP) values. The tree file was then visualized in Figtree v1.4.3 (Rambaut, 2009).

For critical nodes with poorly supported values, we quantified the phylogenetic conflicts among different plastid loci following the methods of Shen et al. (2017), Zhang et al. (2020) and Xiao et al. (2020). A constrained tree search was performed via the ‘-g’ option in IQ-TREE (Nguyen et al., 2015) to obtain the ML trees supporting three different topologies. The site-wise log-likelihood differences for the three constrained ML trees were calculated via the ‘-f G’ option in RAxML v8.2.1 (Stamatakis, 2014). The site-wise values were finally converted to locus-wise log-likelihood differences in R v3.6.2 (R Core Team, 2018).

Divergence time estimation

Rate heterogeneity and topological conflicts across genes can cause model mis-specification in divergence time estimates. To avoid this, we used the SortaDate package (Smith et al., 2018) to filter most clock-like gene regions out from coding and non-coding genes. This method was based on three criteria: (1) clock-likeness; (2) reasonable tree length; and (3) least topological conflict with a focal species tree (Smith et al., 2018). The most clock-like gene regions were concatenated to estimate the divergence time using BEAST v1.10.4 (Suchard et al., 2018): the birth–death tree prior was used with the uncorrelated log-normal (UCLN) relaxed molecular clock. We ran 100 million generations of MCMC and sampled every 1000 generations. Convergence was assessed using TRACER v1.7.1 (Rambaut et al., 2018), based on the likelihood of the ESS exceeding 200 for each parameter. The maximum clade credibility (MCC) tree was generated after discarding the initial 25 % of trees with TREEANNOTATOR v1.10.4 (Suchard et al., 2018). Moreover, the median nodal heights and the age estimation 95 % confidence time intervals were displayed using Figtree v1.4.3 (Rambaut, 2009).

The earliest fossils of Magnoliaceae are from the mid-Cretaceous (Friis et al., 2011). The selection of fossils considered in this study mostly corresponds to that described by Nie et al. (2008). Many Cretaceous fossils of Magnoliaceae may be closely related to *Liriodendron* rather than to extant Magnolioideae (Friis et al., 2011). The oldest fossil seed (*Liriodendroidea alata* Frumin & Friis) of Magnoliaceae, which is similar to extant *Liriodendron* seeds, was assigned to the Cenomanian–Turonian (100.5–93.9 Ma) and was collected in north-western Kazakhstan. Another probable liriodendroid fossil (i.e. *Achaeanthus*) was described from the Dakota Formation (latest Albian–earliest Cenomanian: approx. 100.5 Ma) (Friis et al., 2011; Huang et al., 2020). The observed fossils were hence assigned to the crown age of the family based on a log-normal prior distribution with $\mu = 0.01$, $\sigma = 1$ and an offset of 93.9 Ma: they roughly matched the range of 93.9–100.5 Ma (called ‘Calibration A’ hereafter).

The second robust fossil within Magnoliaceae [*Magnolia latahensis* (Berry) Brown] considered in this study was found in the Clarkia fossiliferous beds in Idaho, USA (Miocene, 17–20 Ma). This was morphologically similar to *Magnolia grandiflora* L. and was grouped in the same clade as *M. grandiflora* and *M. guatemalensis* Donn. Sm. through the phylogeny analysis of *ndhF* sequence data (Golenberg et al., 1990; Kim et al., 2004). The fossil calibration was previously conducted by Nie et al. (2008) to calibrate the genus *Magnolia*. Nie et al. (2008) assigned the calibration point to the crown age of *M. section Magnolia* (corresponding also to the age of *M. grandiflora* and *M. guatemalensis*). Those authors applied a normal distribution, while we applied a log-normal prior distribution. In particular, we considered $\mu = 0.01$, $\sigma = 0.6$ and an offset of 17 Ma to yield a 95 % credible interval (CI) of 17–20 Ma (‘Calibration B’ hereafter), which is congruent with the hypothesized age (17–20 Ma).

The oldest fossil wood of *Magnolia* section *Michelia* (i.e. *Michelia oleifera* Suzuki) has been reported from the Oligocene in the Tsuyazaki Formation, Japan (Suzuki, 1976). A newly discovered mummified fossil wood (of the species *Magnolia nanningensis* Huang, Jin & Oskolski) has also been reported from the upper Oligocene (approx. 23.03 Ma) in South China (Huang et al., 2020). This fossil belongs to *M. subgenus Yulania* (Huang et al., 2020), but cannot be ascribed to any extant species within *M. section Michelia*. The two fossils described above were then used as the third fossil calibration point, which was assigned to the stem age of *M. section Michelia* based on a log-normal distribution ($\mu = 0.01$, $\sigma = 1.21$ and offset = 23.03 Ma), roughly matching the range 33.9–23.03 Ma (‘Calibration C’ hereafter).

Here, we implemented four strategies to test whether the fossil selection criteria greatly affected our dating results: divergence time estimates were achieved by using (1) the three above fossil calibrations (A + B + C), (2) only the oldest fossil taxa of Magnoliaceae and *M. nanningensis* (A + C), (3) only the oldest fossil taxa of Magnoliaceae and *M. latakensis* (A + B) (as in Nie *et al.*, 2008) and (4) only the first calibration point (A) (which constrained the crown age of Magnoliaceae). More details are available in [Supplementary data Table S2](#).

Ancestral geographical range analysis

The extant distribution of *M.* section *Michelia* was obtained from Flora of China (Xia *et al.*, 2008), the Chinese Virtual Herbarium (CVH; <http://www.cvh.ac.cn/>) and the Global Biodiversity Information Facility (GBIF; <https://www.gbif.org/>). Based on Wu *et al.* (2011), two regions were defined: (1) the sub-tropics (including Sino-Japan and Sino-Himalaya) and (2) the tropics (including the southern Yunnan, Guangxi and Hainan provinces in China, as well as Indochina, southern India, Sri Lanka and the Malay Archipelago).

The BioGeoBEARS package (Matzke, 2013), implemented in RASP 4 (Yu *et al.*, 2015), was used to infer the ancestral distribution of *M.* section *Michelia*. Notably, the MCC tree previously generated with BEAST was used as the input tree in the Dispersal-Extinction-Cladogenesis (DEC), Dispersal Vicariance-Analysis (DIVALIKE) and Bayesian inference of historical biogeography for discrete areas (BAYAREALIKE) models (which included the parameter *J*, or ‘jump dispersal’) in both independent and dependent runs. The model selection was accomplished based on the AICc and AICc weights (AICc_wt).

Diversification rate analyses

To estimate the diversification rate shifts, we used the Bayesian analysis in the macroevolutionary mixtures (BAMM) program v.2.5 (Rabosky *et al.*, 2014), although this method remains controversial (Moore *et al.*, 2016; Meyer and Wiens, 2018; Meyer *et al.*, 2018). BAMM explores many candidate models of lineage diversification by applying the reversible jump MCMC method. The MCMC analysis was run for 300 million generations and sampled every 1000 generations based on the MCC tree generated by BEAST. The ‘setBAMMpriors’ function of the ‘BAMMTOOLS’ package in R v3.6.2 (R Core Team, 2018) was chosen to determine the prior values and conduct the post-run analyses. The convergence (ESS > 200) was assessed by plotting the log-likelihood trace of the MCMC output file. The speciation, extinction and net diversification rates were then analysed and plotted using the ‘plotRateThroughTime’ function. These same parameters were also calculated using the RPANDA package v1.9 (Morlon *et al.*, 2016). In this case, the MCC tree sampled from the dating analyses was used to evaluate five time-dependent birth–death models and two null models. Notably, we used the ‘fit_bd’ function to fit the time-dependent birth–death models and then selected the best-fit model based on the AICc values.

In addition, semi-logarithmic lineage-through-time (LTT) plots were calculated using APE v3.5 (Paradis *et al.*, 2004), and 1000 random trees from the converged BEAST trees were used to calculate the 95 % CI.

Notably, the choice of the sampling method can strongly impact the diversification estimates: a moderately incomplete sampling in BAMM was found to provide the most robust estimates (Sun *et al.*, 2020). To avoid the impacts of biased sampling among clades on any diversification inference during the BAMM, RPANDA and LTT analyses, we only included a moderately sampled group [i.e. 33 out of the 57 sampled species (approx. 58 %) were assigned to *M.* section *Michelia* subsection *Michelia*] and excluded the other three subsections [which collectively were represented by four out of the 17 (approx. 24 %) sampled species]. In addition, we accounted for the incomplete sampling of the subsection *Michelia* by applying a sampling fraction (Table 1) in BAMM and RPANDA. Although SSE methods (e.g. GeoSSE and BiSSE) have been widely used to estimate the diversification (i.e. speciation and extinction rates) and dispersal rates among traits (e.g. Goldberg *et al.*, 2011; Lagomarsino *et al.*, 2016), they cannot provide the temporal dynamics of the diversification rates and of the dispersal events. Therefore, no SSE methods were used in this study.

In situ diversification and dispersal events through time

BAMM and RPANDA should be used very carefully when inferring shifts in the diversification rates over time, as discussed by previous authors (Moore *et al.*, 2016; Meyer and Wiens, 2018; Meyer *et al.*, 2018). Here, we applied the method of Xu *et al.* (2020) and, based on the results of the ancestral range analysis (Fig. 1), we identified ‘*in situ* diversification events’ in both the tropics and sub-tropics, ‘dispersal events into the sub-tropics’ and ‘dispersal events into the tropics’. When the distribution of descendants was out of their ancestral ranges, we assigned a dispersal event to the ancestral node and identified an *in situ* diversification event. Based on the divergence time CIs [with highest posterior density (HPD) = 95 %], we estimated the maximum number of observed *in situ* diversification events (MDivE) (Klaus *et al.*, 2016) and dispersal events (MDisE) per million years (Xu *et al.*, 2020). We then counted the MDivE or MDisE at the ancestral node for each slice (i.e. per million years). Notably, all the *in situ* diversification and dispersal events were considered to be independent of each other. Finally, the data were smoothed using the Savitzky–Golay method with three sliding windows to avoid an overinterpretation of smoothing.

RESULTS

Phylogenetic inferences

The whole plastid genome matrix (containing one large single-copy region, one small single-copy region and one inverted repeat region) was 142 646 bp, with 73 415 bp corresponding to the protein-coding region matrix and 69 231 bp to the non-coding region matrix. The dataset of the whole plastome matrix was used to reconstruct the phylogenetic trees through

both the ML and BI methods. Since the ML and BI trees yielded almost identical topologies, in [Supplementary data Fig. S1](#) we show the ML tree with the BI PP values based on the whole plastome matrix.

Overall, our phylogenetic analyses demonstrated that *Magnolia* section *Michelia* (Figlar and Nootboom, 2004) is monophyletic and includes four main clades, with full BS and PP, and that it is a sister of *M.* section *Yulania* ([Supplementary data Fig. S1](#)). The relationships between the four subsections were well resolved (BS = 100, PP = 1.00): *M.* section *Michelia* subsections *Michelia* (clade I + clade II) and *Elmerrillia* (clade III) formed a group (BS = 100, PP = 1.00), followed by clade IV, which was composed of *M.* section *Michelia* subsections *Maingola* and *Aromadendron* (BS = 100, PP = 1.00). Relatively short internal branches frequently occurred at the early stage of diversification of the two main clades (i.e. clade II and, especially, clade I) of *M.* section *Michelia* ([Fig. 1](#); [Supplementary data Fig. S1](#)).

Within *M.* section *Michelia* subsection *Michelia*, two main clades (clades I and II) were identified, although the subsection was weakly supported (BS = 42, PP = 0.74, [Supplementary data Fig. S1](#)). Notably, poor relationships could not be resolved based on non-coding or protein-coding datasets (results not shown). The analysis of the phylogenetic conflicts among different plastid loci demonstrated that three of them (i.e. *ndhC-atpE*, *ndhJ-ndhK* and *psaI-ycf4*) had strong but significantly conflicting phylogenetic signals ([Supplementary data Fig. S2](#)).

Divergence time estimation

After searching for the clock-like gene regions, we estimated the divergence time for the whole Magnoliaceae family using the three clock-like regions (i.e. *ycf1*, *rps16-psbK* and *psbM-psbD*) ([Supplementary data Fig. S3](#)). The topology was constrained based on the results of the complete plastome ML analysis.

The (similar) divergence times estimated through three different calibration strategies are listed in [Supplementary data Table S3](#) and [Figs S3–S6](#). A chronogram, created based on the three fossil calibrations (A + B + C; [Fig. 1](#); [Supplementary data Fig. S3](#)), was used for the remaining analyses of this study. Based on the results, the crown age of the family Magnoliaceae was estimated to be 94.86 Ma, with 95 % HPD = 94.93–98.56 Ma; moreover, the crown age of the subfamily Liriodendroidae was 28.75 Ma (95 % HPD = 14.73–45.46 Ma), while that of the subfamily Magnolioideae was 36.04 Ma (95 % HPD = 28.69–46.11 Ma).

The common ancestor of *M.* sections *Michelia* and *Yulania* should have evolved 25.52 Ma (95 % HPD = 23.05–32.85 Ma); furthermore, *M.* section *Michelia* split into two main clades 16.26 Ma (95 % HPD = 11.96–21.69 Ma), suggesting a middle Miocene origin. The division between *M.* section *Michelia* subsections *Maingola* and *Aromadendron* should have occurred instead 12.54 Ma (95 % HPD = 7.67–17.94 Ma), while the divergence of *M.* section *Michelia* subsections *Michelia* and *Elmerrillia* should have occurred 11.49 Ma (95 % HPD = 8.25–15.44 Ma). Furthermore, the split of *M.* section *Michelia* subsection *Michelia* into two subclades should have occurred 10.82 Ma (95 % HPD = 7.76–14.44 Ma), followed by an immediate and symmetrical diversification in each.

Ancestral distribution estimation

The results of the biogeographical model test are shown in [Supplementary data Table S4](#). The DEC+J model with the smallest AICc value and the largest AICc_wt value was identified as the best-fitting model for our data. The ancestral area reconstructions obtained through this model indicated only the most likely states ([Fig. 1](#)). Based on the results, we can infer that *M.* section *Michelia* and its four subsections originated in the tropics in the late Oligocene and middle Miocene, respectively. Notably, the core group of *M.* section *Michelia* (i.e. *M.* section *Michelia* subsection *Michelia*) originated in the tropics.

Diversification analyses

The phylorate plot in BAMM showed a smooth curve, indicating no shifts in the diversification rates of *M.* section *Michelia* subsection *Michelia*. Moreover, the BAMM analyses conducted for each branch of the subsection *Michelia* provided information on their speciation rate dynamics ([Supplementary data Fig. S7](#)): the speciation rates varied from fast (indicated by a warm colour) to slow (indicated by a cool colour); moreover, both the speciation and net diversification rates declined smoothly, while the extinction rates remained constant. These data indicate that the subsection *Michelia* had an early burst. The RPANDA results indicated that the best-fit model was the one in which the speciation rate varied exponentially over time under a constant extinction rate (Model 4, AICc = 158.12, [Supplementary data Table S5](#)). The rates of speciation, extinction and net diversification ([Supplementary data Fig. S8](#)) showed similar patterns in BAMM ([Supplementary data Fig. S7](#)). Finally, the LTT results indicated an accumulation of lineages and the occurrence of a shift approx. 8 Ma ([Supplementary data Fig. S9](#)).

In situ diversification and dispersal events

In situ diversification events in the tropics increased in number until approx. 8 Ma, following a decreasing trend afterwards. Those in the sub-tropics occurred instead mainly at the beginning and peaked (or shifted) after approx. 3 Ma ([Fig. 2](#)). The dispersal events peaked approx. 8–10 Ma out of the tropics, but approx. 3 Ma between the sub-tropics and tropics ([Fig. 2](#)). These results were confirmed when considering only the dynamics of *M.* section *Michelia* subsection *Michelia* ([Supplementary data Fig. S10](#)), indicating that unsampled species of *M.* section *Michelia* subsections *Elmerrillia*, *Maingola* and *Aromadendron* did not essentially impact the dynamic trends detected in this study.

DISCUSSION

In this study, we reconstructed a robust backbone phylogeny of Magnoliaceae, which is identical to that presented by Y. Wang *et al.* (2020). Notably, a close relationship was confirmed between *M.* sections *Michelia* and *Yulania* (Nie *et al.*, 2008; Kim and Suh, 2013; Y. Wang *et al.*, 2020). Furthermore, the tropical origin of *M.* section *Michelia* was dated to the late Oligocene (when it diverged from *M.* section *Yulania*), while

the diversification of the core group (i.e. *M.* section *Michelia* subsection *Michelia*) happened mainly from the late Miocene onwards. The BAMM and RPANDA analyses indicated a smooth decline of the speciation and net diversification rates of *M.* section *Michelia*, while the extinction rates were constant (Supplementary data Figs S7 and S8). A similar scenario was previously reconstructed for *Primulina* (which includes endemic taxa of northern Vietnam and sub-tropical China), which was explained by a combination of global cooling and the onset of the East Asian monsoon (Kong et al., 2017). Although traditional approaches (e.g. BAMM and RPANDA) have been widely applied to determine the diversification rate shifts of animals and plants (e.g. Shi and Rabosky, 2015; Condamine et al., 2019), problems arise when trying to analyse these shifts over time (Moore et al., 2016; Meyer and Wiens, 2018; Meyer et al., 2018). Newly developed approaches based on biogeographic reconstructions proved to be more effective in this

regard (Klaus et al., 2016; Xing and Ree, 2017; Ding et al., 2020; Xu et al., 2020). Here, the MDivE and MDisE (Klaus et al., 2016; Xu et al., 2020) were estimated to reconstruct the evolutionary dynamics of *M.* section *Michelia*. In this way, two pronounced shifts were identified across the evolutionary history of *M.* section *Michelia*: one in the late Miocene (approx. 8 Ma) and another at the Plio–Pleistocene boundary (approx. 3 Ma) (Fig. 2). These dynamics probably reflect drastic environmental changes that occurred over the late Cenozoic.

Two key evolutionary periods for the biome of southern Asia

Four main pieces of evidence indicated the occurrence of diversification rate shifts in the late Miocene. First, we noted very short internal branches among the two main clades (i.e. clades I and II) of *M.* section *Michelia* between 8 and 11 Ma,

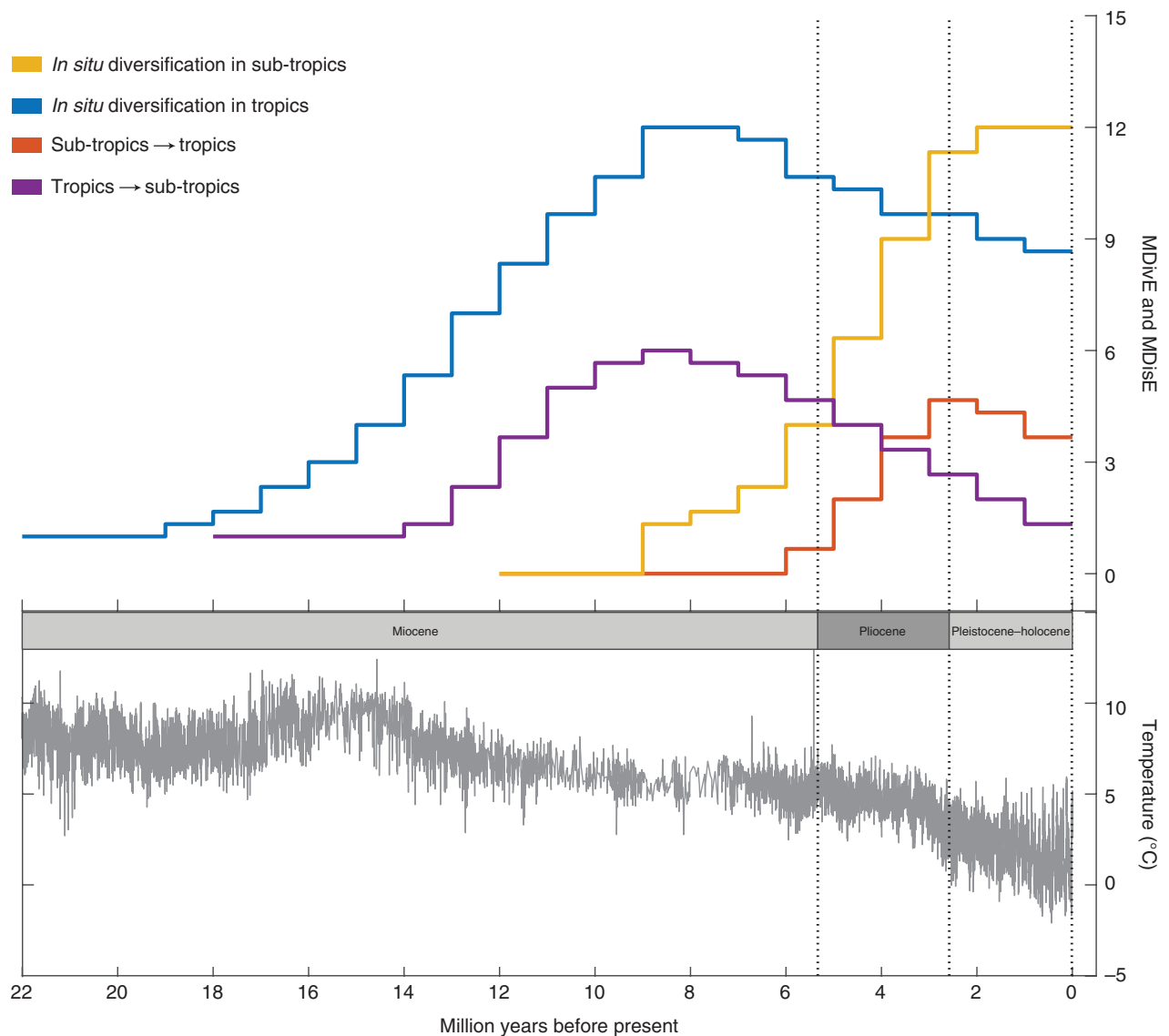


FIG. 2. *In situ* diversification and dispersal rates of *Magnolia* section *Michelia* in the tropics and sub-tropics through time, and global temperature changes through the late Cenozoic (data from Zachos et al., 2008).

indicating a rapid radiation of this section (Supplementary data Fig. S1). The relationships between *M. section Michelia* and its relatives could not be solidly resolved in previous studies (Nie *et al.*, 2008; Kim and Suh, 2013; Y. Wang *et al.*, 2020; Dong *et al.*, 2022). Here, we found that only three plastid regions (i.e. *ndhC-atpE*, *ndhJ-ndhK* and *psaI-ycf4*) have strong and conflicting phylogenetic signals (Supplementary data Fig. S2). This indicates that incomplete lineage sorting (ILS) might play an essential role in the case of rapid radiation. Second, the LTT results demonstrated the occurrence of a great shift approx. 8 Ma (Supplementary data Fig. 9). Third, the peak of dispersal events in the sub-tropics occurred between 8 and 10 Ma (Fig. 2), indicating that the studied taxa lived in a climatically mild environment. Fourth, *in situ* diversification accumulation events shifted from a rapid growth to a gradual decrease since approx. 8 Ma in the tropics (Fig. 2), but kept growing in the sub-tropics. A late Miocene shift in the diversification rates had been previously reconstructed for several plant groups in a similar area of *M. section Michelia* [mainly the family Theaceae (Yu *et al.*, 2017), the *Quercus* section of the subgenus *Cyclobalanopsis*, family Fagaceae (Deng *et al.*, 2018), the *Mahonia* genus, family Berberidaceae (Chen *et al.*, 2020), and the family Lardizabalaceae (W. Wang *et al.*, 2020)]. One of the most remarkable inflections that shaped the biome of southern Asia should have hence occurred in the late Miocene (approx. 8 Ma).

Another drastic shift should have occurred at the Plio–Pleistocene boundary (approx. 3 Ma, Fig. 2): the numbers of *in situ* diversification events in the sub-tropical regions seem to have increased quickly, peaking at the Plio–Pleistocene boundary (Fig. 2). After that time, a higher number of diversification accumulation events was identified in the sub-tropics compared with the tropics (Fig. 2). In addition, we determined a peak in the accumulative dispersal events from the sub-tropical to the tropical regions at the Plio–Pleistocene boundary (approx. 3 Ma, Fig. 2), whereas a sustained decrease of such events was noted in the reverse direction (Fig. 2). Notably, a rapid increase in the diversification rates of Asian tropical and alpine plants has been recognized in the Plio–Pleistocene period (Janssens *et al.*, 2009; Xing and Ree, 2017; Ding *et al.*, 2020), indicating that various biota experienced an elevated diversification rate during that time.

Controls behind the observed dynamic patterns

Three temporally coupled parameters have driven environmental shifts in southern Asia during the late Cenozoic: global cooling, the Tibetan orogenic growth (which involved the Himalaya and the Hengduan Mountains) and the Asian monsoonal regimes (Liu *et al.*, 1998; Tada *et al.*, 2016). Such ecological and environmental shifts influenced the vegetation and plant diversity in the area (Li *et al.*, 2021). For instance, the rapid *in situ* diversification of alpine flora in the Tibet–Himalaya–Hengduan region was profoundly linked to both orogeny and climate change (Xing and Ree, 2017; Ding *et al.*, 2020). Unlike the alpine regions, the southern Asian tropical and sub-tropical regions were mainly and directly impacted by the Asian monsoon and the global climate cooling. Hence, in this study, we considered only these two environmental aspects in relation to the evolution of tropical and sub-tropical biomes.

The two identified evolutionary shifts, which occurred approx. 8 Ma and approx. 3 Ma, coincided temporally with drastic environmental changes (Sun and Wang, 2005; Guo *et al.*, 2008). The occurrence of profound ecological and environmental shifts in Asia in the late Miocene (approx. 8 Ma) is supported by isotopic (Jia *et al.*, 2003), paleomagnetic (An *et al.*, 2001; Guo *et al.*, 2002) and palynological data (Sun and Wang, 2005). Specifically, the environment in these regions shifted from relatively wet to dry in response to an abrupt weakening of the East Asian monsoon approx. 7.5 Ma (Steinke *et al.*, 2010; Clift *et al.*, 2014; Miao *et al.*, 2017). The monsoon intensity gradually decreased, followed by an enhanced variability from approx. 3 Ma onward, which was associated with the start of loess accumulation (Ding *et al.*, 2005) and vegetation changes (Ma *et al.*, 2005; Sun and Wang, 2005) in the Plio–Pleistocene. In particular, global climate cooling alone resulted in landscape drying in the sub-tropics around the world (Herbert *et al.*, 2016, and references therein), in an increase of C_4 plants biomass and in the radiation of succulent lineages in the late Miocene (Cerling *et al.*, 1997; Arakaki *et al.*, 2011).

Decoupling the main causal factors for the dynamic evolutionary patterns observed in this study is difficult, since we did not consider any specific indices for monsoon intensity (i.e. precipitation) and climate cooling (i.e. temperature). However, we can assume that these two factors affected the evolutionary history of *M. section Michelia* in specific ways. In particular, we believe that monsoon intensity played a fundamental role in the evolutionary development of plants. In general, the East Asian monsoon is known to have driven the development of EBLFs (Li *et al.*, 2021). The evolution of *M. section Michelia* (i.e. one of the dominant plants in EBLFs) is expected to have been heavily influenced by this same monsoon, since its first colonization age into sub-tropical areas occurred between the early and middle Miocene (Fig. 1), when modern Asian monsoons intensified (Sun and Wang, 2005; Clift *et al.*, 2014; Farnsworth *et al.*, 2019). In addition, the oldest convincing fossil record of *M. section Michelia* is dated to the late Oligocene (Suzuki, 1976; Huang *et al.*, 2020); our results (to which no fossil calibration was applied; Supplementary data Figs. S5 and S6) and those of other studies (e.g. Nie *et al.*, 2008; Dong *et al.*, 2022) support this conclusion. As a matter of fact, monsoon-like climates in southern Asia would have occurred in the Paleogene (Licht *et al.*, 2014; Spicer *et al.*, 2017; Su *et al.*, 2020; Bhatia *et al.*, 2021), but would have significantly strengthened in the late Oligocene–Early Miocene (25–22 Ma), probably in conjunction with the establishment of the modern Asian monsoon systems (Guo *et al.*, 2002; Sun and Wang, 2005). The Oligocene origin of *M. section Michelia* suggests its diverged adaptation to a wet/warm monsoon environment in southern Asia (Tao, 2000; Herman *et al.*, 2017), while its sister section *Yulania* would have adapted to an arid/cool environment in North-east Asia (Sun and Wang, 2005; Guo *et al.*, 2008). Consequently, we can infer that the occurrence of modern Asian monsoons was fundamental for the origin of *M. section Michelia*.

At the same time, however, the succession of different monsoon climates may have affected other aspects of this section. For instance, we found an exponential growth of diversification events in the sub-tropics over a dry period characterized by a

weakening monsoon (i.e. 8–3Ma) (Clift *et al.*, 2014; Farnsworth *et al.*, 2019). This suggests that the rates of the *in situ* diversification events did not respond positively to the gradual and step-wise weakening of the East Asian monsoon in the late Cenozoic (Fig. 2). *Magnolia* section *Michelia* developed one of its special traits (i.e. the helical thickenings on the vessel walls) as early as in the late Oligocene (Huang *et al.*, 2020). This trait probably allowed this section of tropical origin to adapt to the dry seasons typical of monsoon climates (Huang *et al.*, 2020) and gave it a drought tolerance similar to that of its drought-adaptive relative (i.e. *M. section Yulania*; Liu *et al.*, 2015).

In addition, the patterns of asymmetric dispersal events between the tropics and sub-tropics in both directions suggest that global cooling may have played an important role in the evolution of *M. section Michelia*. It is well known that frequent southward migrations of plants and animals occurred during the Quaternary in the Northern Hemisphere in response to cooling events (e.g. during the occurrence of glacial climate; Hewitt, 2000). In addition, paleovegetation evidence indicates that EBLFs presently inhabiting the sub-tropics and tropics should have retreated southward during the last glacial maximum (Members of China Quaternary Pollen Database, 2000; Yu *et al.*, 2000; Harrison *et al.*, 2001). In this scenario, it is plausible for tropical regions to have received more immigration events detected during the colder period (approx. 3 Ma, Fig. 2): at that time, a global cooling occurred in response to the full establishment of ice sheets in the Northern Hemisphere (Westerhold *et al.*, 2020).

Conversely, a peak of dispersal events out of the tropics occurred approx. 8–10 Ma (Fig. 2), following the tropical conservatism hypothesis (Wiens and Donoghue, 2004). In this view, species that originated in the tropics (e.g. *M. section Michelia* of the family Magnoliaceae) would have been unable to disperse northward (i.e. toward harsher, temperate environments) because of niche conservatism. Global cooling was also proposed as an explanation for the diversification of *Primulina* (based on a best-fitting model; Kong *et al.*, 2017). Overall, it appears that the cooling of the climate below a certain temperature threshold in the late Miocene and late Pliocene may have helped in triggering the observed asymmetric dispersal events between the tropics and sub-tropics.

We acknowledge that unsampled species might have distorted our estimates (e.g. those of the asymmetric dispersal events), but they were unlikely to have overturned them. In fact, an underestimation of both the tropical diversification accumulation events and the patterns of dispersal events in the sub-tropics is unlikely: our sampling fraction (approx. 88 %) in the case of the sub-tropics was relatively high (only four species of the sub-tropics were excluded, Table 1). Meanwhile, the incomplete sampling in the tropics, where the sampling fraction was only approx. 46 % (Table 1), may have led to an underestimation of the tropical diversification and dispersal events between the tropics and sub-tropics. Nonetheless, the patterns of both our estimates (based on the sampling group shown in Fig. 2) agree with that of the limited sampling group (which did not include four tropical species, Supplementary data Fig. S10). This supports the main conclusions of this study: two key shifts and asymmetric dispersal events occurred between the tropical and sub-tropical regions.

Conclusions

In this study, the tropical origin of *M. section Michelia* was dated to the late Oligocene (i.e. when it diverged from *M. section Yulania*). At the same time, the diversification of the core group (i.e. *M. section Michelia* subsection *Michelia*) should have occurred mainly after the late Miocene. Two key shifts (approx. 8 and approx. 3 Ma) were identified and each of them probably recorded a drastic climatic change. Based on our results, it can be inferred that the occurrence of modern Asian monsoons was a fundamental factor for the origin of *M. section Michelia*. The pattern of the asymmetric dispersal events between the tropics and sub-tropics suggests (under the tropical conservatism hypothesis) that the taxa in the two areas probably adapted to global cooling.

Further synthesis studies will be needed to test whether the patterns and hypotheses described in this study can be applied to southern Asia. Overall, we provided a typical example of plants whose evolution reflects past climatic changes in southern Asia. This information might provide unique insights into the effects of ongoing global warming (including biodiversity loss) and suggest possible methods to tackle them.

SUPPLEMENTARY DATA

Supplementary data are available online at <https://academic.oup.com/aob> and consist of the following. Figure S1: phylogeny of the family Magnoliaceae as inferred from the ML analysis of the whole plastid genome sequences. Figure S2: difference of log-likelihood among T1, T2 and T3 for 167 loci. Figure S3: median age estimates of the family Magnoliaceae based on calibration strategy I. Figure S4: median age estimates of the family Magnoliaceae based on calibration strategy II. Figure S5: median age estimates of the family Magnoliaceae based on calibration strategy III. Figure S6: median age estimates of the family Magnoliaceae based on calibration strategy IV. Figure S7: time-dependent speciation, extinction and net diversification rates estimated by BAMM. Figure S8: time-dependent speciation, extinction and net diversification rates estimated by RPANDA. Figure S9: semi-logarithmic lineage-through-time plot for *Magnolia* section *Michelia*. Figure S10: *in situ* diversification and dispersal rates of *Magnolia* section *Michelia* subsection *Michelia* in the tropics and sub-tropics through time. Table S1: information on the samplings conducted for this study. Table S2: fossil calibration strategies applied in this study. Table S3: crown ages estimated for several key nodes and obtained by applying different fossil calibration strategies. Table S4: models for the estimation of the ancestral geographic distributions, which were generated through BioGeoBEARS. Table S5: model selection for the RPANDA analysis.

ACKNOWLEDGEMENTS

We thank Xun Gong, Shou-Zhou Zhang and Ke-Ming Yang for their help with the sampling. We thank Richard B. Figlar for sharing his knowledge of the family Magnoliaceae with us. We are grateful to Wei Xu, Tian-Wen Xiao, Hang-Hui Kong and Yu-Ying Zhou for assisting with the data analyses and laboratory work. Special thanks to Wei Wang, Cristian Roman-Palacios and John J. Wiens for their helpful comments that have contributed to greatly improving the manuscript. Finally,

we would like to thank TopEdit (www.topeditsci.com) for its linguistic assistance during the preparation of this manuscript. The authors have no conflict of interest to declare.

FUNDING

This work was financially supported by the Strategic Priority Research Program of the Chinese Academy of Sciences (grant no. XDB31000000) and the Large-scale Scientific Facilities of the Chinese Academy of Sciences (2017-LSFGBOWS-02) through X.-J.G. and the National Research Foundation of Korea (grant no. NRF-2017R1D1A1B03034952) through S.K.

LITERATURE CITED

- An Z-S, Kutzbach JE, Prell WL, Porter SC. 2001. Evolution of Asian monsoons and phased uplift of the Himalaya–Tibetan plateau since Late Miocene times. *Nature* **411**: 62–66.
- Arakaki M, Christin PA, Nyffeler R, et al. 2011. Contemporaneous and recent radiations of the world's major succulent plant lineages. *Proceedings of the National Academy of Sciences, USA* **108**: 8379–8384. [10.1073/pnas.1100628108](https://doi.org/10.1073/pnas.1100628108)
- Axelrod DI, Al-Shehbaz I, Raven PH. 1996. History of the modern flora of China. In: Zhang AL, Wu SG, eds. *Floristic characteristics and diversity of East Asia Plants*. Beijing: China Higher Education Press and Berlin Heidelberg: Springer-Verlag, 43–55.
- Baldwin BG, Wood KR, Freyman WA. 2021. Directionally biased habitat shifts and biogeographically informative cytonuclear discordance in the Hawaiian silversword alliance (Compositae). *American Journal of Botany* **108**: 2015–2037. [10.1002/ajb2.1757](https://doi.org/10.1002/ajb2.1757)
- Berling DJ, Royer DL. 2011. Convergent Cenozoic CO₂ history. *Nature Geoscience* **4**: 418–420. [10.1038/ngeo1186](https://doi.org/10.1038/ngeo1186)
- Bhatia H, Khan MA, Srivastava G, et al. 2021. Late Cretaceous–Paleogene Indian monsoon climate vis-à-vis movement of the Indian plate, and the birth of the South Asian Monsoon. *Gondwana Research* **93**: 89–100. [10.1016/j.gr.2021.01.010](https://doi.org/10.1016/j.gr.2021.01.010)
- Cerling TE, Harris JM, MacFadden BJ, et al. 1997. Global vegetation change through the Miocene/Pliocene boundary. *Nature* **389**: 153–158. [10.1038/38229](https://doi.org/10.1038/38229)
- Chen X-H, Xiang K-L, Lian L, et al. 2020. Biogeographic diversification of *Mahonia* (Berberidaceae): implications for the origin and evolution of East Asian subtropical evergreen broadleaved forests. *Molecular Phylogenetics and Evolution* **151**: 106910. [10.1016/j.ympev.2020.106910](https://doi.org/10.1016/j.ympev.2020.106910)
- Chen Y-S, Deng T, Zhou Z, Sun H. 2017. Is the East Asian flora ancient or not? *National Science Review* **5**: 920–932.
- Clift PD, Wan S, Blusztajn J. 2014. Reconstructing chemical weathering, physical erosion and monsoon intensity since 25Ma in the northern South China Sea: a review of competing proxies. *Earth-Science Reviews* **130**: 86–102. [10.1016/j.earscirev.2014.01.002](https://doi.org/10.1016/j.earscirev.2014.01.002)
- Condamine FL, Rolland J, Morlon H. 2019. Assessing the causes of diversification slowdowns: temperature-dependent and diversity-dependent models receive equivalent support. *Ecology Letters* **22**: 1900–1912. [10.1111/ele.13382](https://doi.org/10.1111/ele.13382)
- Dawson TP, Jackson ST, House JI, Prentice IC, Mace GM. 2011. Beyond predictions: biodiversity conservation in a changing climate. *Science* **332**: 53–58. [10.1126/science.1200303](https://doi.org/10.1126/science.1200303)
- Deng M, Jiang X-L, Hipp AL, Manos PS, Hahn M. 2018. Phylogeny and biogeography of East Asian evergreen oaks (*Quercus* section Cyclobalanopsis; Fagaceae): insights into the Cenozoic history of evergreen broad-leaved forests in subtropical Asia. *Molecular Phylogenetics and Evolution* **119**: 170–181. [10.1016/j.ympev.2017.11.003](https://doi.org/10.1016/j.ympev.2017.11.003)
- Dierckxsens N, Mardulyn P, Smits G. 2017. NOVOPlasty: de novo assembly of organelle genomes from whole genome data. *Nucleic Acids Research* **45**: e18. [10.1093/nar/gkw955](https://doi.org/10.1093/nar/gkw955)
- Ding W-N, Ree RH, Spicer RA, Xing Y-W. 2020. Ancient orogenic and monsoon-driven assembly of the world's richest temperate alpine flora. *Science* **369**: 578–581. [10.1126/science.abb4484](https://doi.org/10.1126/science.abb4484)
- Ding Z-L, Derbyshire E, Yang S-L, Sun J-M, Liu T-S. 2005. Stepwise expansion of desert environment across northern China in the past 3.5 Ma and implications for monsoon evolution. *Earth and Planetary Science Letters* **237**: 45–55. [10.1016/j.epsl.2005.06.036](https://doi.org/10.1016/j.epsl.2005.06.036)
- Dong S-S, Wang Y-L, Xia N-H, et al. 2022. Plastid and nuclear phylogenomic incongruences and biogeographic implications of *Magnolia* s.l. (Magnoliaceae). *Journal of Systematics and Evolution* **60**: 1–15.
- Farnsworth A, Lunt DJ, Robinson SA, et al. 2019. Past East Asian monsoon evolution controlled by paleogeography, not CO₂. *Science Advances* **5**: eaax1697. [10.1126/sciadv.aax1697](https://doi.org/10.1126/sciadv.aax1697)
- Figlar RB, Nooteboom HP. 2004. Notes on Magnoliaceae IV. *Blumea* **49**: 87–100.
- Friis EM, Crane PR, Pedersen KR. 2011. *Early flowers and angiosperm evolution*. Cambridge: Cambridge University Press.
- Goldberg EE, Lancaster LT, Ree RH. 2011. Phylogenetic inference of reciprocal effects between geographic range evolution and diversification. *Systematic Biology* **60**: 451–465. [10.1093/sysbio/syr046](https://doi.org/10.1093/sysbio/syr046)
- Golenberg EM, Giannasi DE, Clegg MT, et al. 1990. Chloroplast DNA sequence from a Miocene *Magnolia* species. *Nature* **344**: 656–658. [10.1038/344656a0](https://doi.org/10.1038/344656a0)
- Guo Z-T, Ruddiman WF, Hao Q-Z, et al. 2002. Onset of Asian desertification by 22 Myr ago inferred from loess deposits in China. *Nature* **416**: 159–163. [10.1038/416159a](https://doi.org/10.1038/416159a)
- Guo Z-T, Sun B, Zhang Z-S, et al. 2008. A major reorganization of Asian climate by the early Miocene. *Climate of the Past* **4**: 153–174. [10.5194/cp-4-153-2008](https://doi.org/10.5194/cp-4-153-2008)
- Hansen JE, Sato M, Lacis A, Ruedy R, Tegen I, Matthews E. 1998. Climate forcings in the industrial era. *Proceedings of the National Academy of Sciences, USA* **95**: 12753–12758.
- Harrison SP, Yu G, Takahara H, Prentice IC. 2001. Palaeovegetation. Diversity of temperate plants in East Asia. *Nature* **413**: 129–130. [10.1038/35093166](https://doi.org/10.1038/35093166)
- Herbert TD, Lawrence KT, Tzanova A, Peterson LC, Caballero-Gill R, Kelly CS. 2016. Late Miocene global cooling and the rise of modern ecosystems. *Nature Geoscience* **9**: 843–847.
- Herman AB, Spicer RA, Aleksandrova GN, et al. 2017. Eocene–early Oligocene climate and vegetation change in southern China: evidence from the Maoming Basin. *Palaeogeography, Palaeoclimatology, Palaeoecology* **479**: 126–137. [10.1016/j.palaeo.2017.04.023](https://doi.org/10.1016/j.palaeo.2017.04.023)
- Hewitt G. 2000. The genetic legacy of the Quaternary ice ages. *Nature* **405**: 907–913.
- Huang L, Jin J, Quan C, Oskolski AA. 2020. Mummified Magnoliaceae woods from the upper Oligocene of South China, with biogeography, paleoecology, and wood trait evolution implications. *Journal of Systematics and Evolution* **58**: 89–100.
- Janssens SB, Knox EB, Huysmans S, Smets EF, Merckx VSFT. 2009. Rapid radiation of *Impatiens* (Balsaminaceae) during Pliocene and Pleistocene: result of a global climate change. *Molecular Phylogenetics and Evolution* **52**: 806–824. [10.1016/j.ympev.2009.04.013](https://doi.org/10.1016/j.ympev.2009.04.013)
- Jia G-D, Peng P-A, Zhao Q-H, Jian Z-M. 2003. Changes in terrestrial ecosystem since 30 Ma in East Asia: stable isotope evidence from black carbon in the South China Sea. *Geology* **31**: 1093.
- Katoh K, Standley DM. 2013. MAFFT multiple sequence alignment software version 7: improvements in performance and usability. *Molecular Biology and Evolution* **30**: 772–780. [10.1093/molbev/mst010](https://doi.org/10.1093/molbev/mst010)
- Kearse M, Moir R, Wilson A, et al. 2012. Geneious Basic: an integrated and extendable desktop software platform for the organization and analysis of sequence data. *Bioinformatics* **28**: 1647–1649. [10.1093/bioinformatics/bts199](https://doi.org/10.1093/bioinformatics/bts199)
- Kim S, Suh Y. 2013. Phylogeny of Magnoliaceae based on ten chloroplast DNA regions. *Journal of Plant Biology* **56**: 290–305. [10.1007/s12374-013-0111-9](https://doi.org/10.1007/s12374-013-0111-9)
- Kim S, Soltis DE, Soltis PS, Suh Y. 2004. DNA sequences from Miocene fossils: an ndhF sequence of *Magnolia latahensis* (Magnoliaceae) and an rbcL sequence of *Persea pseudocarolinensis* (Lauraceae). *American Journal of Botany* **91**: 615–620. [10.3732/ajb.91.4.615](https://doi.org/10.3732/ajb.91.4.615)
- Klaus S, Morley RJ, Plath M, Zhang Y-P, Li J-T. 2016. Biotic interchange between the Indian subcontinent and mainland Asia through time. *Nature Communications* **7**: 12132.
- Kong H-H, Condamine FL, Harris AJ, et al. 2017. Both temperature fluctuations and East Asian monsoons have driven plant diversification in the karst ecosystems from southern China. *Molecular Ecology* **26**: 6414–6429.
- Kong H, Condamine FL, Yang L, et al. 2022. Phylogenomic and macroevolutionary evidence for an explosive radiation of a plant genus in the Miocene. *Systematic Biology* **71**: 589–609. [10.1093/sysbio/syab068](https://doi.org/10.1093/sysbio/syab068)

- Lagomarsino LP, Condamine FL, Antonelli A, Mulch A, Davis CC. 2016. The abiotic and biotic drivers of rapid diversification in Andean bell-flowers (Campanulaceae). *New Phytologist* **210**: 1430–1442.
- Lanfear R, Frandsen PB, Wright AM, Senfeld T, Calcott B. 2017. PartitionFinder 2: new methods for selecting partitioned models of evolution for molecular and morphological phylogenetic analyses. *Molecular Biology and Evolution* **34**: 772–773. [10.1093/molbev/msw260](https://doi.org/10.1093/molbev/msw260)
- Laslett D, Canback B. 2004. ARAGORN, a program to detect tRNA genes and tmRNA genes in nucleotide sequences. *Nucleic Acids Research* **32**: 11–16. [10.1093/nar/gkh152](https://doi.org/10.1093/nar/gkh152)
- Li H, Durbin R. 2009. Fast and accurate short read alignment with Burrows–Wheeler transform. *Bioinformatics* **25**: 1754–1760. [10.1093/bioinformatics/btp324](https://doi.org/10.1093/bioinformatics/btp324)
- Li H, Handsaker B, Wysoker A, et al. 2009. The Sequence Alignment/Map format and SAMtools. *Bioinformatics* **25**: 2078–2079. [10.1093/bioinformatics/btp352](https://doi.org/10.1093/bioinformatics/btp352)
- Li S-F, Valdes PJ, Farnsworth A, et al. 2021. Orographic evolution of northern Tibet shaped vegetation and plant diversity in eastern Asia. *Science Advances* **7**: eabc7741.
- Licht A, van Cappelle M, Abels HA, et al. 2014. Asian monsoons in a late Eocene greenhouse world. *Nature* **513**: 501–506. [10.1038/nature13704](https://doi.org/10.1038/nature13704)
- Liu H, Xu Q, He P, Santiago LS, Yang K, Ye Q. 2015. Strong phylogenetic signals and phylogenetic niche conservatism in ecophysiological traits across divergent lineages of Magnoliaceae. *Scientific Reports* **5**: 12246. [10.1038/srep12246](https://doi.org/10.1038/srep12246)
- Liu T-S, Zheng M-P, Guo Z-T. 1998. Initiation and evolution of the Asian monsoon system timely coupled with the ice-sheet growth and the tectonic movements in Asia. *Quaternary Sciences* **3**: 194–204.
- Ma Y-Z, Fang X-M, Li J-J, Wu F-L, Zhang J. 2005. The vegetation and climate change during Neocene and Early Quaternary in Jiuxi Basin, China. *Science in China. Series D, Earth Sciences* **48**: 676–688.
- Matzke NJ. 2013. Probabilistic historical biogeography: new models for founder-event speciation, imperfect detection, and fossils allow improved accuracy and model-testing. *Frontiers of Biogeography* **5**: <https://doi.org/10.21425/F5FBG196944>.
- Members of China Quaternary Pollen Database. 2000. Pollen-based biome reconstruction at Middle Holocene (6 ka BP) and Last Glacial Maximum (18 ka BP) in China. *Journal of Integrative Plant Biology* **42**: 1201–1209.
- Meyer ALS, Wiens JJ. 2018. Estimating diversification rates for higher taxa: BAMM can give problematic estimates of rates and rate shifts. *Evolution* **72**: 39–53. [10.1111/evo.13378](https://doi.org/10.1111/evo.13378)
- Meyer ALS, Román-Palacios C, Wiens JJ. 2018. BAMM gives misleading rate estimates in simulated and empirical datasets. *Evolution* **72**: 2257–2266. [10.1111/evo.13574](https://doi.org/10.1111/evo.13574)
- Miao Y, Warny S, Clift PD, Liu C, Gregory M. 2017. Evidence of continuous Asian summer monsoon weakening as a response to global cooling over the last 8 Ma. *Gondwana Research* **52**: 48–58.
- Moore BR, Höhna S, May MR, Rannala B, Huelsenbeck JP. 2016. Critically evaluating the theory and performance of Bayesian analysis of macroevolutionary mixtures. *Proceedings of the National Academy of Sciences, USA* **113**: 9569–9574. [10.1073/pnas.1518659113](https://doi.org/10.1073/pnas.1518659113)
- Morlon H, Lewitus E, Condamine FL, Manceau M, Clavel J, Drury J. 2016. RPANDA: an R package for macroevolutionary analyses on phylogenetic trees. *Methods in Ecology and Evolution* **7**: 589–597.
- Myers N, Mittermeier RA, Mittermeier CG, da Fonseca GAB, Kent J. 2000. Biodiversity hotspots for conservation priorities. *Nature* **403**: 853–858. [10.1038/35002501](https://doi.org/10.1038/35002501)
- Nguyen L-T, Schmidt HA, von Haeseler A, Minh BQ. 2015. IQ-TREE: a fast and effective stochastic algorithm for estimating maximum-likelihood phylogenies. *Molecular Biology and Evolution* **32**: 268–274. [10.1093/molbev/msu300](https://doi.org/10.1093/molbev/msu300)
- Nie Z-L, Wen J, Azuma H, et al. 2008. Phylogenetic and biogeographic complexity of Magnoliaceae in the Northern Hemisphere inferred from three nuclear data sets. *Molecular Phylogenetics and Evolution* **48**: 1027–1040. [10.1016/j.ympev.2008.06.004](https://doi.org/10.1016/j.ympev.2008.06.004)
- Paradis E, Claude J, Strimmer K. 2004. APE: analyses of phylogenetics and evolution in R language. *Bioinformatics* **20**: 289–290. [10.1093/bioinformatics/btg412](https://doi.org/10.1093/bioinformatics/btg412)
- Porebski S, Bailey LG, Baum BR. 1997. Modification of a CTAB DNA extraction protocol for plants containing high polysaccharide and polyphenol components. *Plant Molecular Biology Reporter* **15**: 8–15.
- Qian H. 2002. A comparison of the taxonomic richness of temperate plants in East Asia and North America. *American Journal of Botany* **89**: 1818–1825. [10.3732/ajb.89.11.1818](https://doi.org/10.3732/ajb.89.11.1818)
- Qiu Y-X, Fu C-X, Comes HP. 2011. Plant molecular phylogeography in China and adjacent regions: tracing the genetic imprints of Quaternary climate and environmental change in the world's most diverse temperate flora. *Molecular Phylogenetics and Evolution* **59**: 225–244. [10.1016/j.ympev.2011.01.012](https://doi.org/10.1016/j.ympev.2011.01.012)
- Rabosky DL, Grudler M, Anderson C, et al. 2014. BAMMtools: an R package for the analysis of evolutionary dynamics on phylogenetic trees. *Methods in Ecology and Evolution* **5**: 701–707.
- Rambaut A. 2009. FigTree v1.4.3. <https://ci.nii.ac.jp/naid/10030433668/>. Accessed 1 May 2020.
- Rambaut A, Drummond AJ, Xie D, Baele G, Suchard MA. 2018. Posterior summarization in Bayesian phylogenetics using Tracer 1.7. *Systematic Biology* **67**: 901–904.
- Ramstein G, Fluteau F, Besse J, Joussaume S. 1997. Effect of orogeny, plate motion and land–sea distribution on Eurasian climate change over the past 30 million years. *Nature* **386**: 788–795.
- R Core Team. 2018. R: a language and environment for statistical computing. Vienna, Austria: R Foundation for Statistical Computing.
- Ronquist F, Teslenko M, van der Mark P, et al. 2012. MrBayes 3.2: efficient Bayesian phylogenetic inference and model choice across a large model space. *Systematic Biology* **61**: 539–542. [10.1093/sysbio/sys029](https://doi.org/10.1093/sysbio/sys029)
- Shen X-X, Hittinger CT, Rokas A. 2017. Contentious relationships in phylogenomic studies can be driven by a handful of genes. *Nature Ecology and Evolution* **1**: 0126.
- Shi J-J, Rabosky DL. 2015. Speciation dynamics during the global radiation of extant bats. *Evolution* **69**: 1528–1545. [10.1111/evo.12681](https://doi.org/10.1111/evo.12681)
- Smith SA, Brown JW, Walker JF. 2018. So many genes, so little time: a practical approach to divergence-time estimation in the genomic era. *PLoS One* **13**: e0197433. [10.1371/journal.pone.0197433](https://doi.org/10.1371/journal.pone.0197433)
- Song Y-C, Da L-J. 2016. Evergreen broad-leaved forest of East Asia. In: Box EO, ed. *Vegetation structure and function at multiple spatial, temporal and conceptual scales*. Cham: Springer International Publishing, 101–128.
- Spicer RA. 2017. Tibet, the Himalaya, Asian monsoons and biodiversity – in what ways are they related? *Plant Diversity* **39**: 233–244. [10.1016/j.pld.2017.09.001](https://doi.org/10.1016/j.pld.2017.09.001)
- Spicer R, Yang J, Herman A, et al. 2017. Paleogene monsoons across India and South China: drivers of biotic change. *Gondwana Research* **49**: 350–363. [10.1016/j.gr.2017.06.006](https://doi.org/10.1016/j.gr.2017.06.006)
- Stamatakis A. 2014. RAxML version 8: a tool for phylogenetic analysis and post-analysis of large phylogenies. *Bioinformatics* **30**: 1312–1313. [10.1093/bioinformatics/btu033](https://doi.org/10.1093/bioinformatics/btu033)
- Steinke S, Groeneveld J, Johnstone H, Rendle-Bühning R. 2010. East Asian summer monsoon weakening after 7.5Ma: evidence from combined planktonic foraminifera Mg/Ca and $\delta^{18}O$ (ODP Site 1146; northern South China Sea). *Palaeogeography, Palaeoclimatology, Palaeoecology* **289**: 33–43.
- Su T, Spicer RA, Wu F-X, et al. 2020. A Middle Eocene lowland humid subtropical ‘Shangri-La’ ecosystem in central Tibet. *Proceedings of the National Academy of Sciences, USA* **117**: 32989–32995. [10.1073/pnas.2012647117](https://doi.org/10.1073/pnas.2012647117)
- Suchard MA, Lemey P, Baele G, Ayres DL, Drummond AJ, Rambaut A. 2018. Bayesian phylogenetic and phylodynamic data integration using BEAST 1.10. *Virus Evolution* **4**: vey016. [10.1093/ve/vey016](https://doi.org/10.1093/ve/vey016)
- Sun M, Folk RA, Gitzendanner MA, et al. 2020. Recent accelerated diversification in rosids occurred outside the tropics. *Nature Communications* **11**: 3333. [10.1038/s41467-020-17116-5](https://doi.org/10.1038/s41467-020-17116-5)
- Sun X, Wang P. 2005. How old is the Asian monsoon system? Palaeobotanical records from China. *Palaeogeography, Palaeoclimatology, Palaeoecology* **222**: 181–222.
- Suzuki M. 1976. Some fossil woods from the palaeogene of Northern Kyushu. *The Botanical Magazine* **89**: 59–71.
- Tada R, Zheng H, Clift PD. 2016. Evolution and variability of the Asian monsoon and its potential linkage with uplift of the Himalaya and Tibetan Plateau. *Progress in Earth and Planetary Science* **3**: 4.
- Tang CQ, Matsui T, Ohashi H, et al. 2018. Identifying long-term stable refugia for relict plant species in East Asia. *Nature Communications* **9**: 4488.
- Tao J. 2000. *Evolution of the late Cretaceous–Cenozoic floras in China*. Beijing, China: Science Press.
- Tillich M, Lehwick P, Pellizzer T, et al. 2017. GeSeq—versatile and accurate annotation of organelle genomes. *Nucleic Acids Research* **45**: W6–W11.
- Wambulwa MC, Milne R, Wu Z-Y, et al. 2021. Spatiotemporal maintenance of flora in the Himalaya biodiversity hotspot: current knowledge and future perspectives. *Ecology and Evolution* **11**: 10794–10812. [10.1002/ece3.7906](https://doi.org/10.1002/ece3.7906)

- Wang B, Ho L. 2002.** Rainy season of the Asian–Pacific summer monsoon. *Journal of Climate* **15**: 386–398.
- Wang H-X, Morales-Briones DF, Moore MJ, Wen J, Wang H-F. 2021.** A phylogenomic perspective on gene tree conflict and character evolution in Caprifoliaceae using target enrichment data, with Zabelioideae recognized as a new subfamily. *Journal of Systematics and Evolution* **59**: 897–914.
- Wang P-X. 2004.** Cenozoic deformation and the history of sea–land interactions in Asia. *Geophysical Monograph Series* **149**: 1–22.
- Wang W, Xiang X, Xiang K, Ortiz R del C, Jabbour F, Chen Z. 2020.** A dated phylogeny of Lardizabalaceae reveals an unusual long-distance dispersal across the Pacific Ocean and the rapid rise of East Asian subtropical evergreen broadleaved forests in the late Miocene. *Cladistics* **36**: 447–457.
- Wang Y, Liu B, Nie Z, et al. 2020.** Major clades and a revised classification of *Magnolia* and *Magnoliaceae* based on whole plastid genome sequences via genome skimming. *Journal of Systematics and Evolution* **58**: 673–695. [10.1111/jse.12588](https://doi.org/10.1111/jse.12588)
- Westerhold T, Marwan N, Drury AJ, et al. 2020.** An astronomically dated record of Earth’s climate and its predictability over the last 66 million years. *Science* **369**: 1383–1387. [10.1126/science.aba6853](https://doi.org/10.1126/science.aba6853)
- Wiens JJ, Donoghue MJ. 2004.** Historical biogeography, ecology and species richness. *Trends in Ecology & Evolution* **19**: 639–644.
- Wiens JJ, Graham CH. 2005.** Niche conservatism: integrating evolution, ecology, and conservation biology. *Annual Review of Ecology, Evolution, and Systematics* **36**: 519–539.
- Wu Z-Y, Sun H, Zhou Z-K, Li D-Z, Peng H. 2011.** *Floristics of seed plants from China*. Beijing, China: Science Press.
- Xia N-H, Liu Y-H, Nootboom HP. 2008.** *Magnoliaceae*. In: Wu Z-Y, Raven PH, eds. *Flora of China*. St Louis, USA/Beijing, China: Missouri Botanical Garden Press/Science Press.
- Xiao T-W, Xu Y, Jin L, Liu T-J, Yan H-F, Ge X-J. 2020.** Conflicting phylogenetic signals in plastomes of the tribe Laureae (Lauraceae). *PeerJ* **8**: e10155. [10.7717/peerj.10155](https://doi.org/10.7717/peerj.10155)
- Xing Y, Ree RH. 2017.** Uplift-driven diversification in the Hengduan Mountains, a temperate biodiversity hotspot. *Proceedings of the National Academy of Sciences, USA* **114**: E3444–E3451. [10.1073/pnas.1616063114](https://doi.org/10.1073/pnas.1616063114)
- Xu W, Dong W-J, Fu T-T, et al. 2020.** Herpetological phylogeographic analyses support a Miocene focal point of Himalayan uplift and biological diversification. *National Science Review* **8**: nwa263.
- Ying T-S. 2001.** Species diversity and distribution pattern of seed plants in China. *Biodiversity Science* **9**: 393–398.
- Yu G, Chen X, Ni J, et al. 2000.** Palaeovegetation of China: a pollen database synthesis for the mid-Holocene and last glacial maximum. *Journal of Biogeography* **27**: 635–664. [10.1046/j.1365-2699.2000.00431.x](https://doi.org/10.1046/j.1365-2699.2000.00431.x)
- Yu X-Q, Gao L-M, Soltis DE, et al. 2017.** Insights into the historical assembly of East Asian subtropical evergreen broadleaved forests revealed by the temporal history of the tea family. *New Phytologist* **215**: 1235–1248. [10.1111/nph.14683](https://doi.org/10.1111/nph.14683)
- Yu Y, Harris AJ, Blair C, He X-J. 2015.** RASP (Reconstruct Ancestral State in Phylogenies): a tool for historical biogeography. *Molecular Phylogenetics and Evolution* **87**: 46–49.
- Zachos J, Pagani M, Sloan L, Thomas E, Billups K. 2001.** Trends, rhythms, and aberrations in global climate 65 Ma to present. *Science* **292**: 686–693. [10.1126/science.1059412](https://doi.org/10.1126/science.1059412)
- Zachos JC, Dickens GR, Zeebe RE. 2008.** An early Cenozoic perspective on greenhouse warming and carbon-cycle dynamics. *Nature* **451**: 279–83. [10.1038/nature06588](https://doi.org/10.1038/nature06588)
- Zhang R, Wang Y-H, Jin J-J, et al. 2020.** Exploration of plastid phylogenomic conflict yields new insights into the deep relationships of Leguminosae. *Systematic Biology* **69**: 613–622. [10.1093/sysbio/syaa013](https://doi.org/10.1093/sysbio/syaa013)